ARTICLE
Journal of Cellular Biochemistry 117:694–707 (2016)

Journal of Cellular Biochemistry

# Monocyte Chemoattractant Protein-Induced Protein 1 Overexpression Modulates Transcriptome, Including MicroRNA, in Human Neuroblastoma Cells

Elżbieta Boratyn,[1] Iwona Nowak,[1] Irena Horwacik,[1] Małgorzata Durbas,[1] Anna Mistarz,[1] Magdalena Kukla,[2] Przemysław Kaczówka,[1] Maria Łastowska,[3] Jolanta Jura,[2] and Hanna Rokita[1]*

[1]*Laboratory of Molecular Genetics and Virology, Faculty of Biochemistry, Biophysics and Biotechnology, Jagiellonian University, Gronostajowa 7, Kraków 30-387, Poland*

[2]*Department of General Biochemistry, Faculty of Biochemistry, Biophysics and Biotechnology, Jagiellonian University, Gronostajowa 7, Kraków 30-387, Poland*

[3]*Department of Pathology, Institute "Pomnik – Centrum Zdrowia Dziecka", Aleja Dzieci Polskich 20, Warszawa 04-730, Poland*

## ABSTRACT

The recently discovered MCPIP1 (monocyte chemoattractant protein-induced protein 1), a multidomain protein encoded by the *MCPIP1* (*ZC3H12A)* gene, has been described as a new differentiation factor, a ribonuclease, and a deubiquitination-supporting factor. However, its role in cancer is poorly recognized. Our recent analysis of microarrays data showed a lack of expression of the MCPIP1 transcript in primary neuroblastoma, the most common extracranial solid tumor in children. Additionally, enforced expression of the *MCPIP1* gene in BE(2)-C cells caused a significant decrease in neuroblastoma proliferation and viability. Aim of the present study was to further investigate the role of MCPIP1 in neuroblastoma, using expression DNA microarrays and microRNA microarrays. Transient transfections of BE(2)-C cells were used for overexpression of either wild type of MCPIP1 (MCPIP1-wt) or its RN-ase defective mutant (MCPIP1-ΔPIN). We have analyzed changes of transcriptome and next, we have used qRT-PCR to verify mRNA levels of selected genes responding to MCPIP1 overexpression. Additionally, protein levels were determined for some of the selected genes. The choline transporter, CTL1, encoded by the *SLC44A1* gene, was significantly repressed at the specific mRNA and protein levels and most importantly this translated into a decreased choline transport in MCPIP1-overexpressing cells. Then, we have found microRNA-3613-3p as the mostly altered in the pools of cells overexpressing the wild type MCPIP1. Next, we analyzed the predicted targets of the miR-3613-3p and validated them using qRT-PCR and western blot. These results indicate that the expression of miR-3613-3p might be regulated by MCPIP1 by cleavage of its precursor form. J. Cell. Biochem. 117: 694–707, 2016.


**KEY WORDS:** NEUROBLASTOMA; MONOCYTE CHEMOATTRACTANT PROTEIN-INDUCED PROTEIN 1 (*ZC3H12A*); PIN DOMAIN; EXPRESSION MICROARRAYS; microRNA

The recently discovered MCPIP1 (monocyte chemoattractant protein-induced protein 1), a multidomain protein encoded by the *MCPIP1* (*ZC3H12A)* gene, also known as regnase-1, has so far been described as a new differentiation factor [Vrotsos et al., 2009], a ribonuclease [Matsushita et al., 2009; Skalniak et al., 2009; Lipert et al., 2014], and a deubiquitination-supporting factor [Wang et al., 2015]. Its major role in immune system as a negative regulator of inflammation has been described [Jura et al., 2012]. The *MCPIP1*

Abbreviations: C-, control; M-, MCPIP1-wt; P-, MCPIP1-ΔPIN.

Conflicts of interest: None.

Grant sponsor: Polish National Science Center; Grant number: 2011/03/B/NZ1/00024; Grant sponsor: Research Project Competition for Young Researchers and PhD Students of the Faculty of Biochemistry, Biophysics and Biotechnology Jagiellonian University; Grant number: 1/2014.

*Correspondence to: Prof. Dr. Hanna Rokita, Laboratory of Molecular Genetics and Virology, Faculty of Biochemistry, Biophysics and Biotechnology, Jagiellonian University, Gronostajowa 7, 30-387 Kraków, Poland.
E-mail: hanna.rokita@uj.edu.pl

Manuscript Received: 10 July 2015; Manuscript Accepted: 24 August 2015

Accepted manuscript online in Wiley Online Library (wileyonlinelibrary.com): 26 August 2015

DOI 10.1002/jcb.25354 • © 2015 Wiley Periodicals, Inc.

gene can be activated by such proinflammatory cytokines as IL-1β, TNFα, and the chemoattractant protein - MCP-1 as well as LPS and PMA. However, it also appears to be a post-transcriptional suppressor of cytokines expression and, therefore, plays a role in inhibition of inflammation [Mizgalska et al., 2009]. Moreover, the MCPIP1 protein participates in deubiquitination of TRAF proteins, leading to a decrease in activity of the NF-κB pathway and silencing of inflammatory reactions [Jura et al., 2012].

The PIN (RNase) domain of MCPIP1 has been determined by Mizgalska et al. [2009], and its direct involvement in IL-1β and MCPIP1 mRNA degradation appears to be independent of the presence of ARE (AU-rich elements) in the 3′UTR. MCPIP1 controls also the level of IL-6, IL-12p40, and IL-2 transcripts [Matsushita et al., 2009; Li et al., 2012]. Moreover, MCPIP1 constitutes a key regulator of adipogenesis [Lipert et al., 2014]. Additionally, a dual activity of human MCPIP1, which could be attributed to its RNase domain, was found in a hepatoma cell line infected with hepatitis C virus, one involving direct degradation of viral RNA and the other, encompassing degradation of the virus-induced expression of mRNAs of proinflammatory cytokines, such as TNFα, IL-6, and MCP-1 [Lin et al., 2014]. MCPIP1 can also restrict HIV-1 production in $CD4^+$ T-cells by decreasing the levels of viral mRNAs through its RNase activity, thus creating a potent barrier against HIV-1 infection at a posttranscriptional level [Liu et al., 2013].

A role of MCPIP1 in cancer is not thoroughly recognized. It was shown that MCPIP1 overexpression decreased constitutive activity of NF-κB and limited the survival of HeLa cells [Skalniak et al., 2013]. It is widely known that elevated constitutive activity of NF-κB is one of the mechanisms providing increased survival of cancer cells; therefore, death-promoting properties of MCPIP1 in a proteasome inhibitor MG-132-treated HeLa cells may derive from the negative effect of MCPIP1 on the constitutive NF-κB activity [Skalniak et al., 2014]. On the other hand, deubiquitinase activity of MCPIP1 was found to be responsible for stabilization of the RGS2 protein (Regulator of G protein signalling 2), a suggested tumor suppressor, in breast cancer cells [Lyu et al., 2015].

MicroRNAs constitute a novel class of regulatory molecules, influencing stability, and/or translational availability of mRNAs [Zhi et al., 2014]. The microRNA pathway usually involves Drosha and Dicer ribonuclease complexes necessary for processing of primary microRNAs [Stroynowska-Czerwińska et al., 2014]. A number of expression profiling studies have demonstrated dysregulation of miRNAs in neuroblastoma [Zhi et al., 2014]. Differential patterns of microRNA expression in neuroblastoma are correlated with prognosis, differentiation, and apoptosis [Chen and Stallings, 2007]. It was found that some epigenetically silenced miRNAs targeted genes were overexpressed in tumors from patients with poor survival as well as in cell lines. Moreover, it has been recently shown, that MCPIP1 can cleave the terminal loops of precursor miRs, and this anti-Dicer activity can suppress miRNA and endo-siRNA biogenesis [Suzuki et al., 2011]. MCPIP1 upregulation by several proinflammatory stimuli, including IL-1β and MCP-1, might be partly attributable to global miRNA downregulation found in cancer, in addition to reduced expression of Dicer and Drosha [Suzuki et al., 2011].

Our recent analysis of microarrays data showed a lack of expression of the MCPIP1 transcript in primary neuroblastoma, the most common extracranial solid tumor in children. Enforced *MCPIP1* gene expression in BE(2)-C cells caused a significant decrease in neuroblastoma proliferation and viability [Skalniak et al., 2014a]. To continue our study on the role of MCPIP1 in neuroblastoma, we applied high-throughput analytical methods such as DNA and microRNA microarrays to analyze changes in gene expression of BE(2)-C human neuroblastoma cells with overexpression of the *MCPIP1* gene and identify genes involved in the MCPIP1 pathway.

## MATERIALS AND METHODS

### CELL CULTURE AND GENETIC CONSTRUCTS

Cell culture of BE(2)-C cells (ATCC, CRL-2268) and the genetic constructs were previously described in details [Mizgalska et al., 2009; Skalniak et al., 2014a]. Briefly, BE(2)-C cells were cultured at 37 °C, in a 5% $CO_2$ atmosphere in a mixture of the Eagle′s Minimum Essential Medium (Sigma–Aldrich) and the F12 medium (Sigma–Aldrich) (1:1) supplemented with 10% fetal calf serum (Gibco), 1% non-essential amino acid solution, 1 mM sodium pyruvate, and 50 μg/ml gentamicin (complete medium) (all obtained from Sigma–Aldrich). Plasmids were isolated with Qiagen Plasmid Purification Midi Kit (Qiagen), according to the manufacturer′s protocol and checked for quality by cutting with restriction enzymes followed by electrophoresis in an agarose gel (1%), visualized by SimplySafe™ ($EUR_X$), according to the manufacturer′s protocol.

### TRANSFECTION OF THE BE(2)-C HUMAN NEUROBLASTOMA CELL LINE

For overexpresion of MCPIP1, the human neuroblastoma cell line BE (2)-C was transfected with genetic constructs. For this purpose, cells were seeded at a density of 30,000/$cm^2$ in complete medium. After 1 day of culture, the cell medium was changed, and cells were transfected with one of the constructs or green fluorescent protein (GFP), as previously described [Skalniak et al., 2014a]. For transfection, PEI (polyethylenimine) (Sigma-Aldrich) was used according to the standard recommendations, with a PEI:DNA ratio of 3:1 prepared in Opti-MEM medium (Gibco). The medium containing the transfection mix was removed and replaced by fresh complete medium 7 h after transfection. After transfection, BE(2)-C cells were cultured in complete medium supplemented with geneticin (Lab Empire, G418) at a concentration of 800 μg/ml, which was added to the culture medium since day 1 after transfection. The medium containing G418 was refreshed every day, until the fourth day after transfection when the cells were collected. The expression of the construct was determined by western blot and RT-PCR.

### RNA ISOLATION, RT-PCR, AND QUANTITATIVE RT-PCR

RNA isolation from transfected cells followed by cDNA production was performed as described previously [Horwacik et al., 2013]. For the semiquantitative RT-PCR and quantitative RT-PCR experiments, 1 μg of total RNA has been reverse transcribed. Following the synthesis, non-diluted cDNA was amplified using GenAmp (Perkin

Elmer) thermocycler and DyNAzyme$^{TM}$II (Thermo Fisher) polymerase. For qRT-PCR, the Eco (Illumina) system and KAPA SYBR FAST qPCR Master Mix (Kapa Biosystems) were used and cDNA was diluted 20–100 times. For the normalization of each sample, the amount of eukaryotic translation elongation factor 2 (*EF2*) cDNA was measured. For RT-PCR and qRT-PCR, the previously described primers for *EF2* gene were used [Skalniak et al., 2014a], product size 214 bp, annealing temperature 62 °C. For qRT-PCR, also previously described primers were used for the following genes: *MBNL2* [Hernández-Hernández et al., 2013], *TPX2* [Grover et al., 2012], *MCM10* [Kaur et al., 2012], *DICER* [Jafari et al., 2013], *APAF1* [Robles et al., 2001], *DFFB* [Jansen et al., 2003], *NF1* [Xu et al., 2014], and *RORA* [Odawara et al., 2009]. Other primers were designed using Primer-BLAST (http://www.ncbi.nlm.nih.gov/tools/primer-blast/). Sequences of primers from 5′ to 3′ end are listed below. For RT-PCR following primers were used: *MCPIP1* F:GCCTCCACTCCCAGAAGAG, R: GCTCATCTGCCACAGAGCG, product size 644 bp if cells were transfected with wild-type MCPIP1 and product size 170 bp if cells were transfected with MCPIP1 without the PIN domain, annealing temperature 57 °C. For qRT-PCR following primers were used: *CTXN1* F: GTGTTCGCCTTCGTGCTCT, R: ACCAACGCGTAGTCGAACTG; *CNIH2* F: GCCTTCTACCTGCTCTCCTTC, R: TTGGGGGTTGGAGAGGCT; *SLC44A1* F: GACCGTAGCTGCACAGACAT, R: ATACATACTTCCGCTGGGTGTG; *CD248* F: ACTACGTTGGTGGCTTCGAG, R: CCCGTCATCCAGCAACTCAT, *ARRB1* F: GGAGAACCCATCAGCGTCAA, R: GGGCACTTGTACTGAGCTGT, *RBM12* F: ATGTGGAAGTTAGCCCTGCC, R: GTCTGAGGAGGGGGATGAGT *C16ORF53 (PAXIP1)* F: CCCAGAGCGAAGAGGAGAGA, R: GTCCTTTGGTGTCACTGGCT; *SEPT3* F: TGGGGGATCATCGAAGTGGA R: TCGTGGCTTTCCTCTGTGTC; S*LC29A4* F: CTACTTTGCGATGCTGCTGG, R: ATGGAGGTCCCTGGGTACTTG, *SLC3A2* F: TACTCCCAACTACCGGGGTG, R: CCGCAATCAAGAGCCTGTC; *SLC35E2* F: GGTGACTTTCAGGTCCCGCA, R: GAGAGCGGCCACTTTTCCT; *KIF3A* F: AGCCCAACAAGAGCATCAGTC, R: ACAAGTCAACCCCACCAACA; *MAP3K1* F: GGTAATCACACAGGAAGAGAAACT, R: ATTCTCCATCTCACGACGACA. Quantification was performed using the "ΔΔCt" relative quantitation method. Experiments were performed at least three times in triplicates.

## GENE EXPRESSION PROFILING

Total RNA was isolated using the TRI Reagent according to the manufacturer's instructions. Next, gene expression profiling was performed by Genbioinfo. RNA concentration was measured using a ND-1000 Spectrometer (NanoDrop Technologies, Inc.). RNA quality was determined using an Agilent Bioanalyzer 2100 (Agilent). A starting amount of 200 ng of high-quality total RNA was used to generate cDNA and cRNA with the Illumina TotalPrep RNA amplification kit (Illumina). The procedure consisted of RT with an oligo(dT) primer bearing a T7 promoter using Array-Script. The obtained cDNA became a template for in vitro transcription with T7 RNA polymerase and biotin UTP, which generated multiple copies of biotinylated cRNA. The purity and concentration of the cRNA were determined using a NanoDrop ND-1000 Spectrometer. Quality cRNA was subsequently hybridized using a direct hybridization array kit (Illumina). Each cRNA sample (1.5 μg) was hybridized overnight using the HumanHT-12 BeadChip array (Illumina) in a multiple-step procedure; the chips were washed, dried, and scanned on the BeadArray Reader (Illumina). Raw microarray data were generated using BeadStudio v3.0 (Illumina). A total of 12 Illumina HumanHT-12v3 microarrays were used in the experiment. Microarray data analysis and quality control were performed using BeadArray R package v1.0.0. After background subtraction (using median background method), the data were normalized using quintile normalization and were subsequently $\log_2$-transformed. The obtained signal was taken as the measure of mRNA abundance derived from the level of gene (or particular transcriptional form) expression. The expression values were standardized to reduce variation between the experimental batches. One-way ANOVA was applied to calculate significance levels (*P*-values) to discriminate differentially expressed genes between the groups (control, MCPIP1-wt, and MCPIP1-ΔPIN). The false discovery rate was estimated using the Benjamini and Hochberg method. All statistical analyses were performed using R software version 2.10.1. Hierarchical clustering was performed with dChip software using Euclidean distance and average linkage method.

## MicroRNA MICROARRAYS

Total RNA was isolated using the *mir*Vana$^{TM}$ miRNA isolation kit (Life Technologies) according to the manufacturer's instructions. The microRNA gene expression profile was obtained from Exiqon, based on triple RNA samples isolated by us from cells expressing either the wild type MCPIP1 or the mutant, devoid of the RNase domain. The quality of the total RNA was verified by an Agilent 2100 Bioanalyzer profile. 750 ng total RNA from both sample and reference was labeled with Hy3$^{TM}$ and Hy5$^{TM}$ fluorescent label, respectively, using the miRCURY LNA$^{TM}$ microRNA Hi-Power labeling kit, Hy3$^{TM}$/Hy5$^{TM}$ (Exiqon) following the procedure described by the manufacturer. The Hy3$^{TM}$-labeled samples and a Hy5$^{TM}$-labeled reference RNA sample were mixed pair-wise and hybridized to the miRCURY LNA$^{TM}$ microRNA Array 7th Gen (Exiqon), which contains capture probes targeting all microRNAs for human, mouse, or rat registered in the miRBASE 18.0. The hybridization was performed according to the miRCURY LNA$^{TM}$ microRNA array instruction manual using a Tecan HS4800$^{TM}$ hybridization station (Tecan). After hybridization, the microarray slides were scanned and stored in an ozone-free environment (ozone level below 2.0 ppb) in order to prevent potential bleaching of the fluorescent dyes. The miRCURY LNA$^{TM}$ microRNA array slides were scanned using the Agilent G2565BA Microarray Scanner System (Agilent Technologies, Inc., Santa Clara, CA) and the image analysis was carried out using the ImaGene® 9 (miRCURY LNA$^{TM}$ microRNA Array Analysis Software, Exiqon). The quantified signals were background corrected (Normexp with offset value 10) and normalized using the global Lowess (locally weighted scatterplot smoothing) regression algorithm.

## MiRNA REAL-TIME QUANTITATIVE RT-PCR

100 ng of RNA was reverse transcribed in triplicate in the total reaction volume of 10 μl using miRCURY LNA$^{TM}$ Universal RT microRNA PCR (Exiqon). Following the synthesis, cDNA was diluted 80 times and assayed in 10-μl PCR reactions according to the manufacturer's protocol for miRCURY LNA Universal RT microRNA

PCR (Exiqon). Selected miRNA was assayed once by qRT-PCR using Eco (Illumina) system. All negative and positive controls recommended by manufacturer were performed. For the normalization of each sample, the amount of U6 cDNA was measured. All primers were provided by Exiqon.

### PROTEIN EXTRACTS ISOLATION AND WESTERN BLOT ANALYSES

The cells ($1 \times 10^6$/per well) were grown on 6-well plates. Whole cell extracts were obtained according to the TRI reagent method (Lab Empire), or using RIPA buffer (25 mM Tris-HCl pH 7.6, 150 mM NaCl, 1% sodium deoxycholate, 0.1% SDS) supplemented with halt phosphatase cocktail (Thermo Scientific) and complete (Roche). The protein content in cell extracts was measured using BCA method [Smith, 1985]. Proteins were resolved using SDS-PAGE, followed by western blotting as described previously in details [Horwacik et al., 2013; Skalniak et al., 2014a]. Methods of isolation of proteins, amounts of protein lysates, and concentrations of particular antibodies used for western blotting were optimized empirically. Following, primary antibodies were used; anti-MCPIP1 was purchased from Sigma (SAB3500391; 1:1,000), or kindly provided by Dr. Jacek Jura (these antibodies were used in 1 μg/ml concentration). The antibody against GAPDH was purchased from Sigma (G8795; 1:40,000); against SLC44A1 (CTL1) (MBS851525; 1:1,000) was from MyBioSource; against APAF1 (#8723; 1:1,000), against Dicer (#5362; 1:1,000), and against α-tubulin (#2125S; 1:1,000) was from Cell Signaling Technology; against DFFB (ab71083; 1:1,000) and against NF1 (ab17963; 1:1,000) was purchased from Abcam, and against RORα (sc-6062; 1:200) was purchased from Santa Cruz Biotechnology. Secondary HRP conjugate antibodies were from Cell Signaling Technology: goat anti-rabbit IgG (#7074; 1:2,000) and Sigma–Aldrich: rabbit anti-mouse IgG antibodies (A-9044; 1:40,000). Samples were normalized using reference signal from binding of the anti-GAPDH or anti-α tubulin antibodies.

### [$^3$H]-CHOLINE UPTAKE INTO BE(2)-C CELLS

[Methyl-$^3$H]-choline chloride (specific activity: 80 Ci/mmol, concentration: 1 mCi/ml) was obtained from Hartmann Analytical Gmbh. Non-transfected cells were seeded at a density of 30,000/cm$^2$ on 24-well culture plates. Transfected cells were seeded on the third day after transfection at a density of 40,000/cm$^2$ on 24-well culture plates. On the next day after seeding cells were washed with PBS and uptake buffer (122 mM NaCl, 4.9 mM KCl, 1.3 mM $CaCl_2$, 15.8 mM $Na_2HPO_4$, 1,2 mM $MgSO_4$, 11 mM glucose, containing the appropriate concentration of unlabeled choline) was added to each well. The [$^3$H]-choline stock solution was diluted 1:40 with the uptake buffer without unlabeled choline. The uptake was started by the addition to wells of diluted [$^3$H]-choline as described by Ray et al. [2009]. After incubation in 37 °C with shaking, cells were washed twice with ice-cold PBS and dissolved in 100 μl of RIPA buffer and aliquots were taken for liquid scintillation counting using liquid scintillation cocktail (Perkin Elmer) and protein concentration was determined using the BCA method. Radioactivity was measured with a Wallac WinSpectral 1414 Liquid Scintillation Counter (Perkin Elmer) system. The specific uptake of [$^3$H]-choline was calculated as the difference between total [$^3$H]-choline uptake in the presence and absence of 30 mM unlabeled choline. The values of $V_{max}$ and $K_m$ were calculated by creating secondary, reciprocal plot, according to the Lineweaver–Burk linearization substrate-velocity method from the mean values of measurements deriving from three experiments.

### STATISTICAL ANALYSES

Data on graphs and in Table I were presented as means ± SEM (a standard error of the mean). All experiments were repeated at least three times. We applied series of pairwise tests (*t*-test), comparing, e.g., means of control and transfected cells with following *P*-values: $P < 0.05$ (*), $P < 0.01$ (**), $P < 0.001$ (***).

## RESULTS

### ENFORCED *MCPIP1* GENE EXPRESSION IN BE(2)-C HUMAN NEUROBLASTOMA CELLS

Our former studies have revealed a very low expression of the *MCPIP1* gene in human neuroblastoma cell lines and a lack of expression in primary neuroblastoma tumors [Skalniak et al., 2014a]. To further explore a role of MCPIP1 in neuroblastoma, we have generated pools of BE(2)-C neuroblastoma cells with transient overexpression of the gene, its wild type form (MCPIP1-wt), and an RNase domain deficient mutant (MCPIP1-ΔPIN) (Fig. 1). Enforced expression of *MCPIP1* lasted till the fourth day in culture (Fig. 1A) with the transcript level increased ca sevenfold over control (over 10-fold for the mutant, devoid of the RN-ase domain) (Fig. 1C). Higher levels of the mutant form of the transcript and consequently of the mutated protein could be explained by lack of self-degradation of its own transcript as it was found for the wild type MCPIP1 [Mizgalska et al., 2009]. The protein level showed, respectively, ca four- and sixfold increase, for the wild type and the mutant gene (Fig. 1D). It should be emphasized that endogenous MCPIP1 expression is negligible (Fig. 1C, D). Transfection efficiency was at the level of ~ 50%, as evaluated by fluorescent microscopy in cells transfected with the same vector containing the green fluorescence protein (GFP) gene sequence (Fig. 1B) and an effect of the overexpressed mutant form being comparable with the control cells.

TABLE I. The Most Differentially Expressed miRNAs in BE(2)-C Human Neuroblastoma Cells

| miRNA | MCPIP1wt/control ratio | *P*-value |
|---|---|---|
| miR-3613-3p | 0.330 | $1{,}74 \times 10^{-9}$ |
| miR-4668 | 0.364 | $6{,}18 \times 10^{-8}$ |
| miR-3613-5p | 1.879 | $1{,}61 \times 10^{-2}$ |
| miR-1275 | 0.538 | $1{,}61 \times 10^{-2}$ |
| miR-675-5p | 0.547 | $2{,}03 \times 10^{-2}$ |
| miR-4787-5 | 0.560 | $2{,}60 \times 10^{-2}$ |
| miR-3146 | 0.560 | $2{,}60 \times 10^{-2}$ |
| miR-3201 | 0.566 | $2{,}99 \times 10^{-2}$ |

The list of differentially expressed microRNAs is shown. The arrays were performed in quadruplicates. Fold change in expression of miRs in MCPIP1 overexpressing cells versus control cells transfected with empty plasmid is presented. *P*-values mean statistical significance.

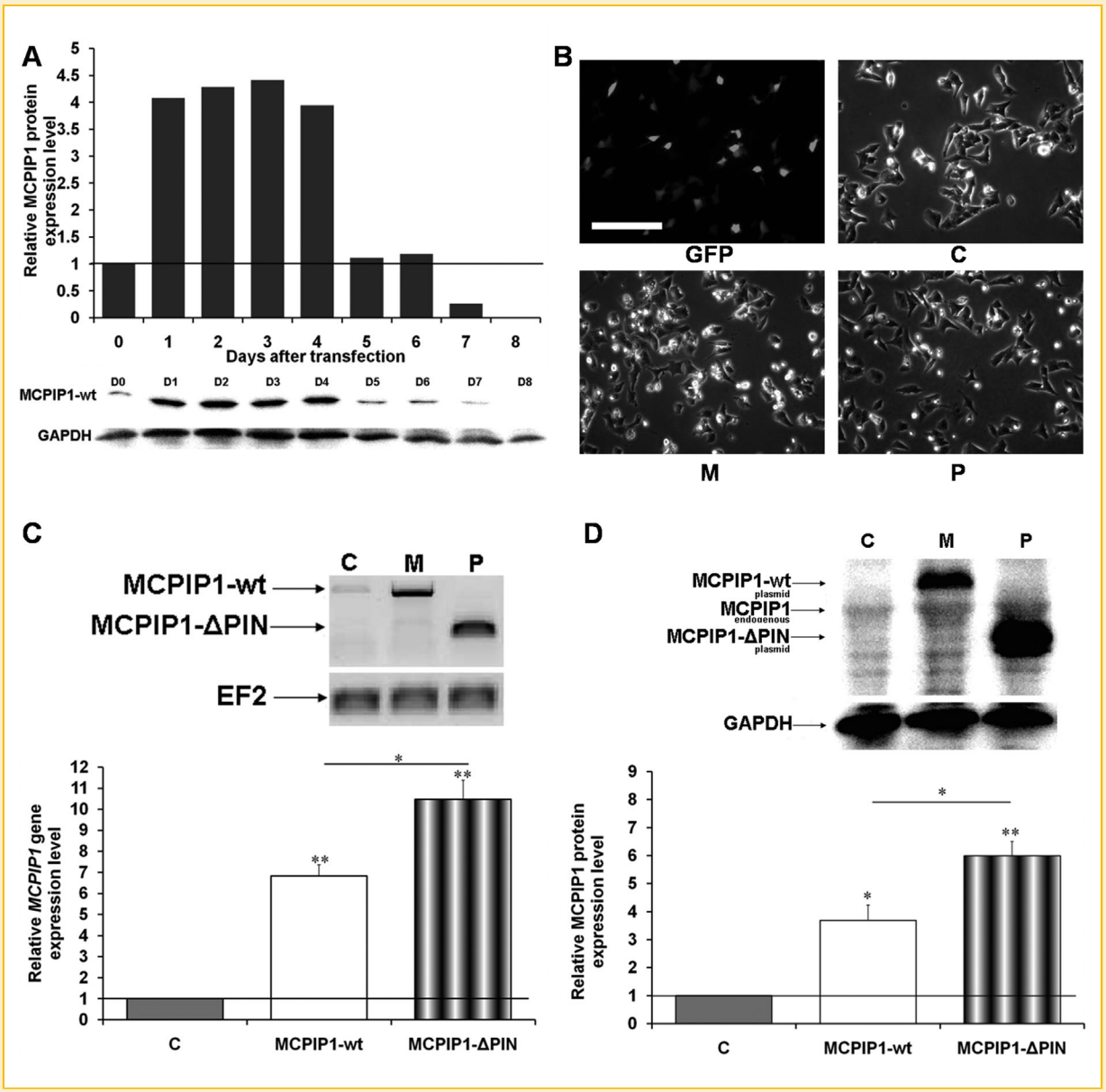


**Fig. 1.** Overexpression of the MCPIP1 in human neuroblastoma cells. A: kinetics of MCPIP1 protein expression in BE(2)-C cells. MCPIP1 protein was measured by western blot in whole cell protein extracts from BE(2)-C cells 0–8 days after transfection. GAPDH protein expression was used as reference. Experiment was performed one time. B: microscopic observation of control (C), expressing wild type MCPIP1-wt (M), mutant form of MCPIP1–MCPIP1-ΔPIN (P), and green fluorescent protein (GFP) cells (scale bar, 200 μm). Cells were taken at 20× magnification using a Leica DM IRE2 microscope with a Leica DC350 SX digital camera. C: *MCPIP1* mRNA content measured by RT-PCR with *EF2* as a reference, in BE(2)-C pools of cells expressing either wild type or mutant MCPIP1. The results are mean values of four separate experiments ± SEM. D: MCPIP1 protein (with GAPDH protein as a reference) content in BE(2)-C pools of cells expressing either wild type or mutant MCPIP1 was measured by western blot in whole cell protein extracts ± SEM. Experiments were performed four times. All shown photographs were representative. *P*-values for *t*-test (control vs. MCPIP1-wt or MCPIP1-ΔPIN and MCPIP1-wt vs. MCPIP1-ΔPIN) were $P < 0.05$ (*), $P < 0.01$ (**). *P*-values for *t*-test MCPIP1-wt versus MCPIP1-ΔPIN are underlined.

## DIFFERENTIALLY EXPRESSED GENES IN DISTINCT POOLS OF MCPIP1-EXPRESSING NEUROBLASTOMA CELLS

We have applied microarray methodology to characterize possible changes in expression of genes affected by the studied RNase. Expression microarray analysis was performed on samples isolated from BE(2)-C cells with overexpression of the wild type and the mutant MCPIP1. Microarray data analysis using one-way ANOVA allowed identification of 127 differentially expressed genes ($P < 1 \times 10^{-4}$, FDR < 5%). A total of 12 transcripts exhibited more than 1.3-fold differences between the analyzed groups (Fig. 2). All transcripts levels, except those of *MBNL2* and *TPX2*, were decreased (*CTXN1*, *CNIH2*, *SLC44A1*, *CD248*, *ARRB1*, *RBM12*, *PAXIP1*, *SEPT3*, *MCM10*, and *SLC29A4*). Quantitative RT-PCR analysis of the most changed genes in BE(2)-C cells transiently overexpressing

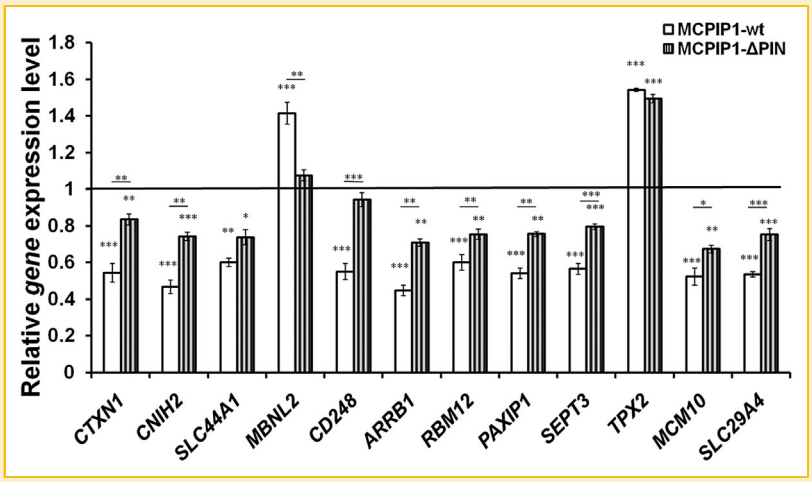


**Fig. 2.** DNA microarray analysis of the selected genes in MCPIP1 overexpressing neuroblastoma cells. Diagram – relative gene expression levels for 12 selected genes are presented. *P*-values for *t*-test (control vs. MCPIP1-wt or MCPIP1-ΔPIN and MCPIP1-wt vs. MCPIP1-ΔPIN) were $P < 0.05$ (*), $P < 0.01$ (**), $P < 0.001$ (***). *P*-values for *t*-test MCPIP1-wt versus MCPIP1-ΔPIN are underlined.

MCPIP1 confirmed the microarray data for the majority of the genes except *TPX2*, which was only insignificantly increased for the wild type form and *ARRB1*, which was not decreased (Figs. 3 and 4A, D). qRT-PCR of the described set of genes in BE(2)-C cells overexpressing the mutant *MCPIP1* revealed less pronounced changes with only one exception of *TPX2* (Fig. 3).

Based on the results, we were able to select several interesting genes for further analyses. Moreover, *MCM10*, *CD248*, and *RBM12* from the group of five mostly inhibited genes are expressed in all six human neuroblastoma cell lines (CHP134, IMR-32, NMB, TR14, SKNFI and SK-N-SH) (Łastowska M. – personal communication). Therefore, expression of MCPIP1 could have its inhibitory effect on other neuroblastoma cell lines, not only BE(2)-C cell line, studied by us.

## MCPIP1 OVEREXPRESSION DECREASES CHOLINE TRANSPORT IN NEUROBLASTOMA CELLS

The solute carrier 44A1 (SLC44A1), also known as choline transporter-like protein 1 (CTL1), is a recently discovered choline transporter [Michel and Bakovic, 2012]. Choline is an essential nutrient required to phosphatidylcholine and acetylcholine biosynthesis as well as it serves as an important donor of methyl groups. Human CTL1 is expressed in a variety of tissues including brain, heart, small intestine, kidney, liver, skeletal muscle, pancreas, spleen, ovary, and testis [Michel and Bakovic, 2012]. Enhanced choline transport is implicated in the pathogenesis of multiple disorders and certain cancers such as breast and ovarian cancer [Iorio et al., 2005]. An aberrant activation of the PI3K/AKT/mTOR pathway in human lung adenocarcinoma might be involved in the cancer proliferation and was shown to regulate choline transport, as the specific pathway inhibitors blocked [$^3$H]-choline uptake [Wang et al., 2007]. Our expression microarray analysis has revealed significant decrease in *SLC44A1* gene product content in human neuroblastoma cells overexpressing the MCPIP1 protein (Fig. 4). Quantitative RT-PCR and western blot analyses have confirmed the microarray data and have shown significant decrease in the *SLC44A1* mRNA and CTL1 protein level (Fig. 4D, E). Interestingly, neuroblastoma cells overexpressing the mutant MCPIP1 form, have also shown diminished *SLC44A1* mRNA and protein levels, which implies that the RN-ase domain of the MCPIP1 might not be solely responsible for the inhibition of the choline transporter expression. Additionally, we examined the time-course of [$^3$H]-choline uptake at concentration of 10 nM in BE(2)-C cells for 90 min. [$^3$H]-choline uptake increased in a time-dependent manner and it was linear with time upto ca 40 min (data not shown). We have demonstrated that the choline transporter function is decreased in cells overexpresing MCPIP1 protein, as uptake of [$^3$H]-choline was profoundly inhibited in the cells as compared with control cells (Fig. 4F). A kinetic analysis of [$^3$H]-choline specific uptake enabled calculation of a Michaelis–Menten constant ($K_m$) and maximal velocity ($V_{max}$) which were respectively 5.24 μM and 0.240 pmol/μg protein/min for control cells, 6.33 μM and 0.228 pmol/μg protein/min for MCPIP1wt-expressing cells, and 9.96 μM and 0.166 pmol/μg protein/min for the mutant form-expressing cells (Fig. 4G). Thus, the decrease of maximal rate of choline uptake was measured in MCPIP1-wt- and MCPIP1-ΔPIN-expressing cells, with more pronounced change for the mutant form-expressing cells, while the $K_m$ values were slightly enhanced in the cells overexpressing MCPIP1-wt and more clearly enhanced in the cells overexpressing MCPIP1-ΔPIN. It could be concluded that the RNase domain of the MCPIP1 protein plays a role in choline uptake.

Three other transporters were affected by MCPIP1 overexpression – *SLC29A4*, the plasma membrane monoamine transporter (PMAT) gene [Adamsen et al., 2014] (Fig. 4A), and *SLC35E2*, an uncharacterized transporter gene showing lower expression of the transcript in unfavourable neuroblastoma tumors (a suggested marker of malignancy in neuroblastoma) [Thorell et al., 2009] (Fig. 4C), were inhibited at their mRNA levels. The *SLC3A2* gene encoding, a part of sodium-independent cystine:glutamate exchanger System Xc [Giraudi et al.,

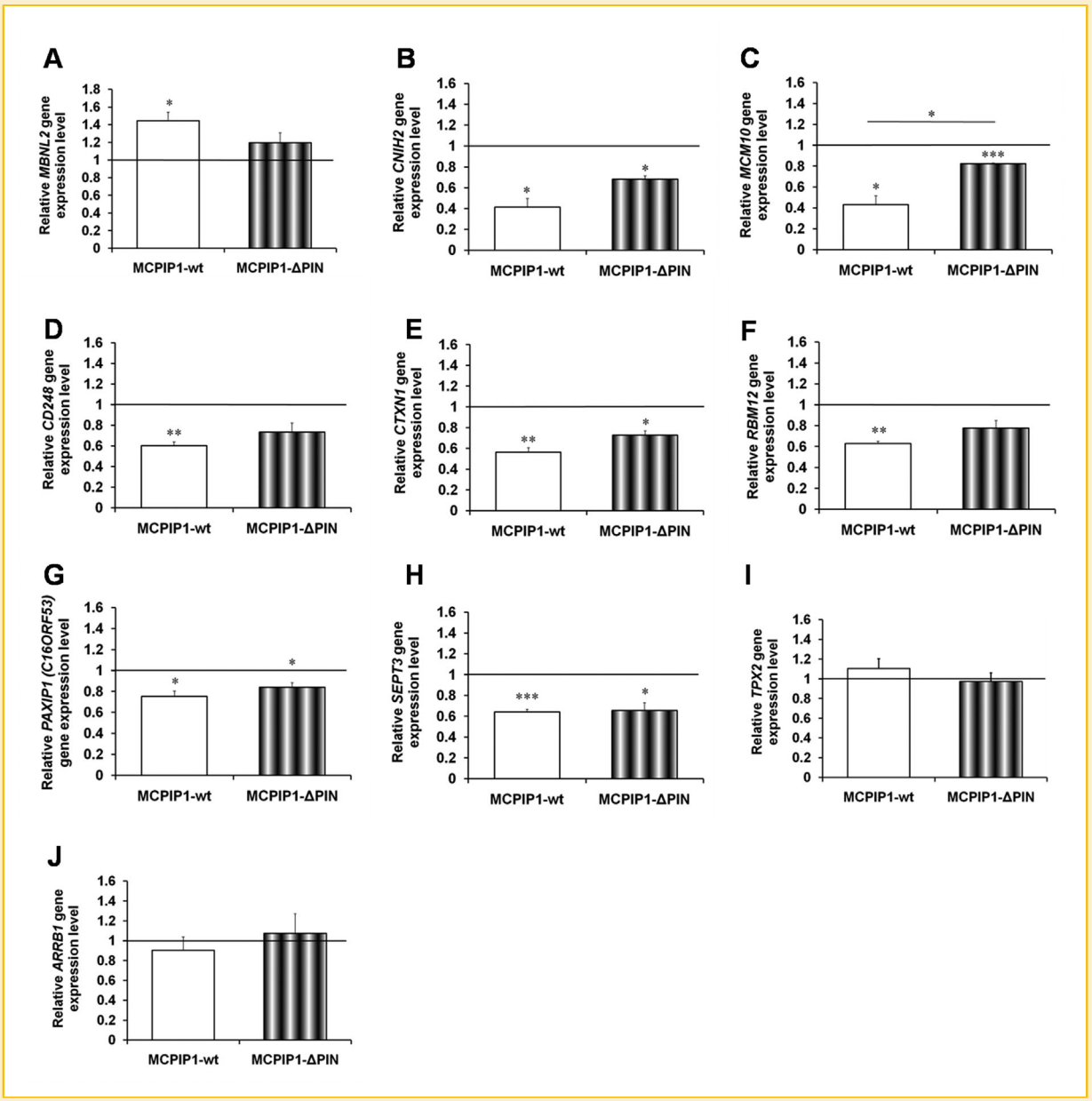


**Fig. 3.** Quantitative RT-PCR analysis of the most changed genes in BE(2)-C cells overexpressing MCPIP1. Relative *MBNL2* (A), *CNIH2* (B), *MCM10* (C), *CD248* (D), *CTXN1* (E), *RBM12* (F), *PAXIP1* (*C16ORF53*) (G), *SEPT3* (H), *TPX2* (I), *ARRB1* (J) genes expression levels in BE(2)-C pools of control, expressing either wild type (MCPIP1-wt) or mutant MCPIP1 (MCPIP1-ΔPIN) cells were shown. The EF2 gene expression level was used as a reference. Experiments were performed at least three times in triplicates. Data on the graphs are presented as means ± SEM and calculated versus control values, set as 1 (black baseline). *P*-values for *t*-test (control vs. MCPIP1-wt or MCPIP1-ΔPIN and MCPIP1-wt vs. MCPIP1-ΔPIN) were $P < 0.05$ (*), $P < 0.01$ (**), $P < 0.001$ (***). *P*-values for *t*-test MCPIP1-wt versus MCPIP1-ΔPIN are underlined.

2011; Guo et al., 2015], was increased (Fig. 4B). Induction of the System Xc in SH-SY5Y neuroblastoma cells renders the cell less prone to oxidative damage [Giraudi et al., 2011].

### ANALYSIS OF DIFFERENTIALLY EXPRESSED MIRNAS IN DISTINCT POOLS OF MCPIP1-EXPRESSING NEUROBLASTOMA CELLS AND THEIR POTENTIAL TARGETS

We have continued our gene expression study and performed the microRNA profiling on RNA samples obtained from BE(2)-C cells overexpressing the wild type and the mutant forms of *MCPIP1*. We identified a subset of eight microRNA candidates (out of the total number of 774 microRNAs analyzed by the miRCURY LNA™ microRNA Array), which were differentially expressed in MCPIP1-wt-transfected cells and the *P*-value was less than 0.05 (Fig. 5) (Table I). As the lowest *P*-value was assigned to two miRNAs, i.e., miR-3613-3p and miR-4668, their content was determined by qRT-PCR. The method confirmed the changes in the miR-3613-3p expression level and showed that the wild-type form of the MCPIP1

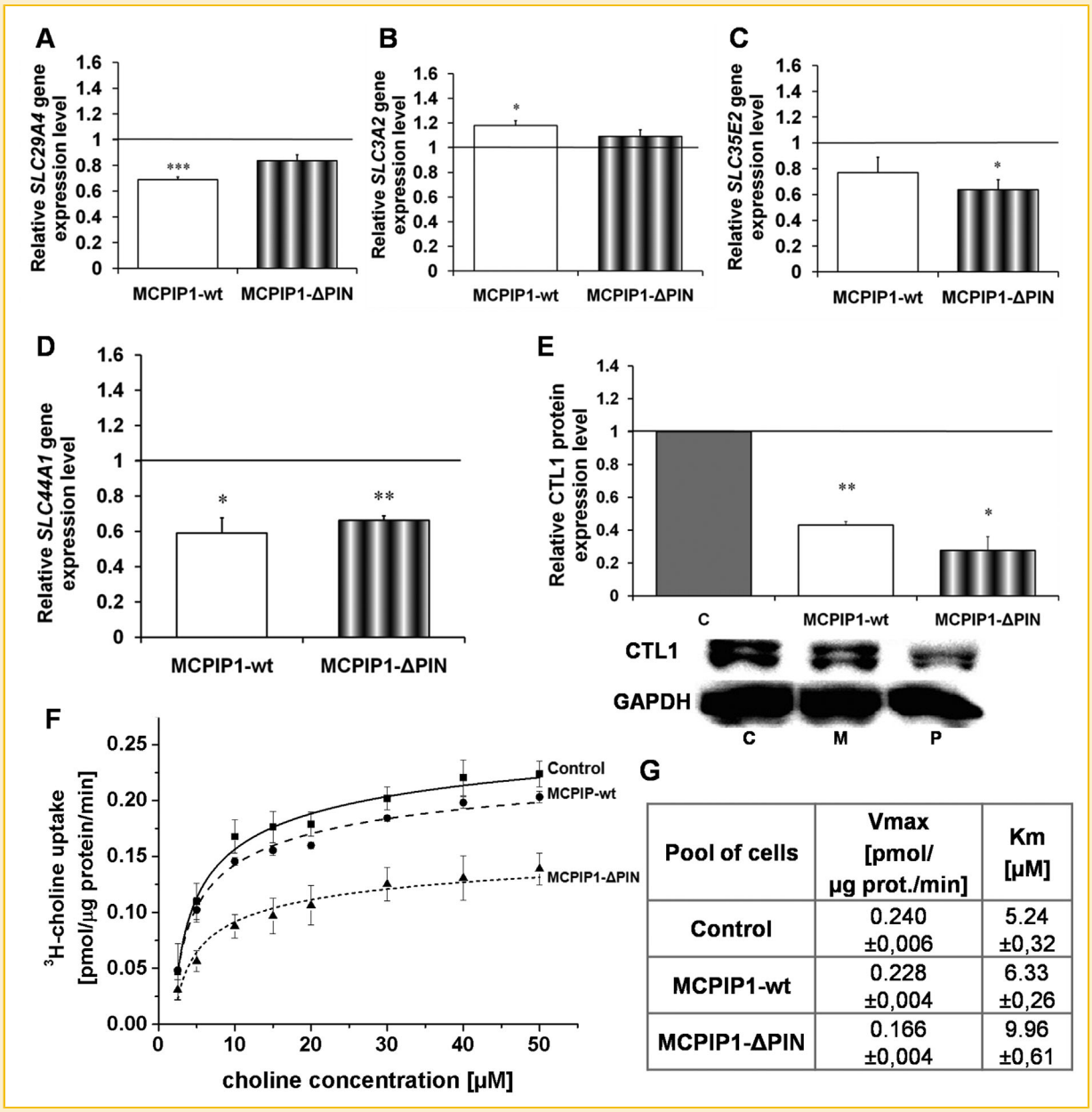


| Pool of cells | Vmax [pmol/ µg prot./min] | Km [µM] |
|---|---|---|
| Control | 0.240 ±0,006 | 5.24 ±0,32 |
| MCPIP1-wt | 0.228 ±0,004 | 6.33 ±0,26 |
| MCPIP1-ΔPIN | 0.166 ±0,004 | 9.96 ±0,61 |

**Fig. 4.** Expression of selected members of SLC family of transporters in human neuroblastoma BE(2)-C cells overexpressing MCPIP1. Relative *SLC29A4* (A), *SLC3A2* (B), *SLC35E2* (C), and *SLC44A1* (D) genes expression levels were measured with quantitative RT-PCR. The EF2 gene expression level was used as a reference. Experiments were performed at least three times in triplicates. E: relative CTL1 protein expression level was measured with western blot. The GAPDH protein expression was used as a reference. Experiments were performed four times. Data on the graphs A–E are presented as means ± SEM and calculated versus control values, set as 1 (the black baseline and the gray bar). Western blot result for CTL1 protein is representative. *P*-values for *t*-test (control vs. MCPIP1-wt or MCPIP1-ΔPIN and MCPIP1-wt vs. MCPIP1-ΔPIN) were $P < 0.05$ (*), $P < 0.01$ (**), $P < 0.001$ (***). No significance was found for *t*-test MCPIP1-wt versus MCPIP1-ΔPIN. F: the kinetic characteristic of [$^3$H]-choline uptake. Data on the graph are presented as means ± SEM, experiment was performed three times in duplicates and measurement was performed six times. G: values of $V_{max}$ and $K_m$ for all studied pools of cells (the values were calculated from the equations of regression curves applied to mean values of measurements deriving from three experiments; the errors were calculated based on the fit function parameters using total differential method). All experiments were performed on BE(2)-C pools of control (C), expressing either wild type (MCPIP1-wt or M), or mutant MCPIP1 (MCPIP1-ΔPIN or P) cells.

has significantly decreased the miRNA level (appr. to 50% of control), while the mutated MCPIP1 form (deprived of PIN domain) did not cause significant change in the microRNA content (Fig. 7A). miR-4668 represented a false positive signal in qRT-PCR and was not further studied.

The reliable identification of transcripts that are regulated by miRNAs is essential for delineating the specific functions of miRNAs. Therefore, we performed extensive bioinformatic analysis using the mirDB, T TargetScan, and TargetMiner databases, and found possible mRNA targets binding miR-3613-3p prevalently in their

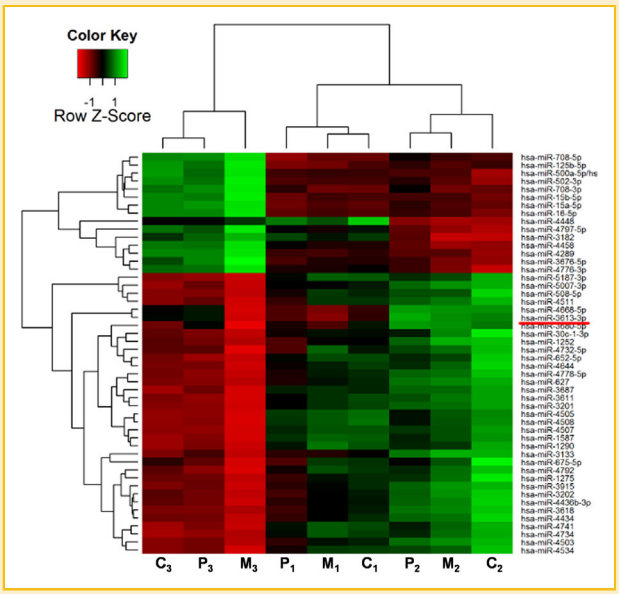


**Fig. 5.** The heat map diagram of a two-way hierarchical clustering of miRNAs and samples from human neuroblastoma BE(2)-C cells overexpressing MCPIP1. The clustering was done using the complete-linkage method together with the euclidean distance measure on all samples performed on BE-(2)-C pools of control ($C_{1-3}$), expressing either wild type ($M_{1-3}$), or mutant MCPIP1 ($P_{1-3}$) cells, and on the top 50 microRNAs with highest standard deviation (miRNA-3613-3p was underlined in red). The miRNA clustering tree is shown on the left. Changes in levels of expression from high to low are indicated by changes in color from green to red.

3′UTRs. We have picked eight likely miR-3613-3p targets due to their presence in at least two databases with high probability value, and their role in neuroblastoma pathogenesis or differentiation of neural cells. Transcripts of the following genes were chosen for further analysis due to low mfe (minimal free energy) values: *DFFB*, *APAF1*, *DICER*, *RORA*, *KIF3A*, *MAP3K1*, *NF1*, and *VHL*. All characteristic features of miRNA:mRNA interaction, i.e., a seed region at 5′ end, a complementary region at 3′ end, and a mismatched bulb region between the ends were found only for RORA and VHL (Fig. 6). Quantitative RT-PCR and western blot analyses suggest that only two of the mRNAs, i.e., DFFB and APAF1, could be a direct targets of the miR-3613-3p (Figs. 7B, C and 8A, B) as their specific mRNA and protein levels have increased with statistical significance in the neuroblastoma cells overexpressing the *MCPIP1* gene. *SLC35E2* (Fig. 4C), *NF1* (Figs. 7F and 8E), *MAP3K1* (Fig. 7G), and *KIF3A* (Fig. 7H) might not be targeted by the miR-3613-3p, since their specific mRNA and/or protein content was either not changed or decreased.

BE(2)-C cells overexpressing the mutant of MCPIP1, which cannot cleave pre-miRNA, presented unchanged level of the miR-3613-3p (Fig. 7A) and expressed the target mRNAs mostly unchanged, further confirming that the observed changes might be caused by the miR-3613-3p. As *KIF3A* and *MAP3K1* mRNAs were respectively either decreased or increased in cells overexpressing the mutant of MCPIP1, it might suggest that the effect is not direct. At the protein level, the data for five of the predicted target mRNAs were less evident as with only one exception found for RORα (Fig. 8D). The other protein levels (DFFB, APAF1, Dicer, and NF1) (Fig. 8A–C, E) were significantly decreased in neuroblastoma cells overexpressing the mutant form of MCPIP1. Again, the effect could be attributed to the other than RNase activity of the MCPIP1 such as a deubiquitinase-binding factor.

## DISCUSSION

Neuroblastoma is a malignant childhood tumor of the sympathetic nervous system with a highly variable prognosis. This form of cancer occurs in 1 in 100,000 children, with 650 new cases each year in the United States. For older children, more that 1.5 years of age, the prognosis is bad and majority of patients with disseminated form of the disease are expected to relapse within 3 years [Ora and Eggert, 2011]. Amplification of the *MYCN* gene found in ca 20% of neuroblastoma tumors confers a poor prognosis and ectopic expression of MYCN in neuroblastoma cell lines was found to stimulate cell cycle progression [Huang and Weiss, 2013]. Through PI3K/mTOR pathway activation, MYCN stimulates expression of vascular endothelial growth factor (VEGF) and new blood vessels for tumor growth [Kang et al., 2008]. Many MYCN-regulated genes encode regulatory RNAs and chromatin structure modifying enzymes. High expression of MYCN might be responsible for inhibition of MCPIP1 expression through silencing of the MCP-1 receptor [Huang and Weiss, 2013]. We have found an inverse correlation between expression patterns of MCPIP1 and MYCN in BE (2)-C human neuroblastoma cells [Skalniak et al., 2014a].

Our microarray analysis reveals a group of proteins prevalently involved in RNA and DNA metabolism. MBNL2 (the muscleblind-like protein 2) is a highly conserved double-stranded RNA-binding protein, interacting with expanded CUG repeats that form extended hairpins in pre-mRNAs and thus disturbing proper splicing [Lee et al., 2013]. MBNL2 participates in the differentiation of neurons, adipocytes, and blood cell types. The MBNL proteins appear to play an important role in pathogenesis of myotonic dystrophy, an RNA-mediated disorder. MBLN2 mediates a brain developmental splicing program and its sequestration by CUGs enriched pre-mRNAs causes adult splicing patterns disruption. It was shown that Mbnl2 loss in knockout mice caused misregulated splicing of hundreds of exons [Lee et al., 2013]. MBNL2 is not expressed in six human neuroblastoma cell lines (CHP134, IMR-32, NMB, TR14, SKNFI, and SKNSH) (Łastowska M. personal communication). Therefore, it could be anticipated that increase in *MBNL2* gene expression found by us in MCPIP1-overexpressing BE(2)-C cells could have its modulatory effect on the neuroblastoma splicing program.

The selected genes encode among others also MCM10, the DNA replication factor minichromosome maintenance complex component 10, a conserved abundant nuclear protein crucial for initiation of eukaryotic DNA replication [Okorokov et al., 2007]. The MCM10 molecule is recruited to replication origins to provide a link between MCM2-7 complex DNA helicase and DNA polymerases. It is suggested that MYCN might stimulate the initiation of DNA replication and G1-S-phase transition by induction of the minichromosome maintenance complex [Koppen et al., 2007]. In neuroblastoma, MCM10 is a target of MYCN [Koppen et al., 2007],

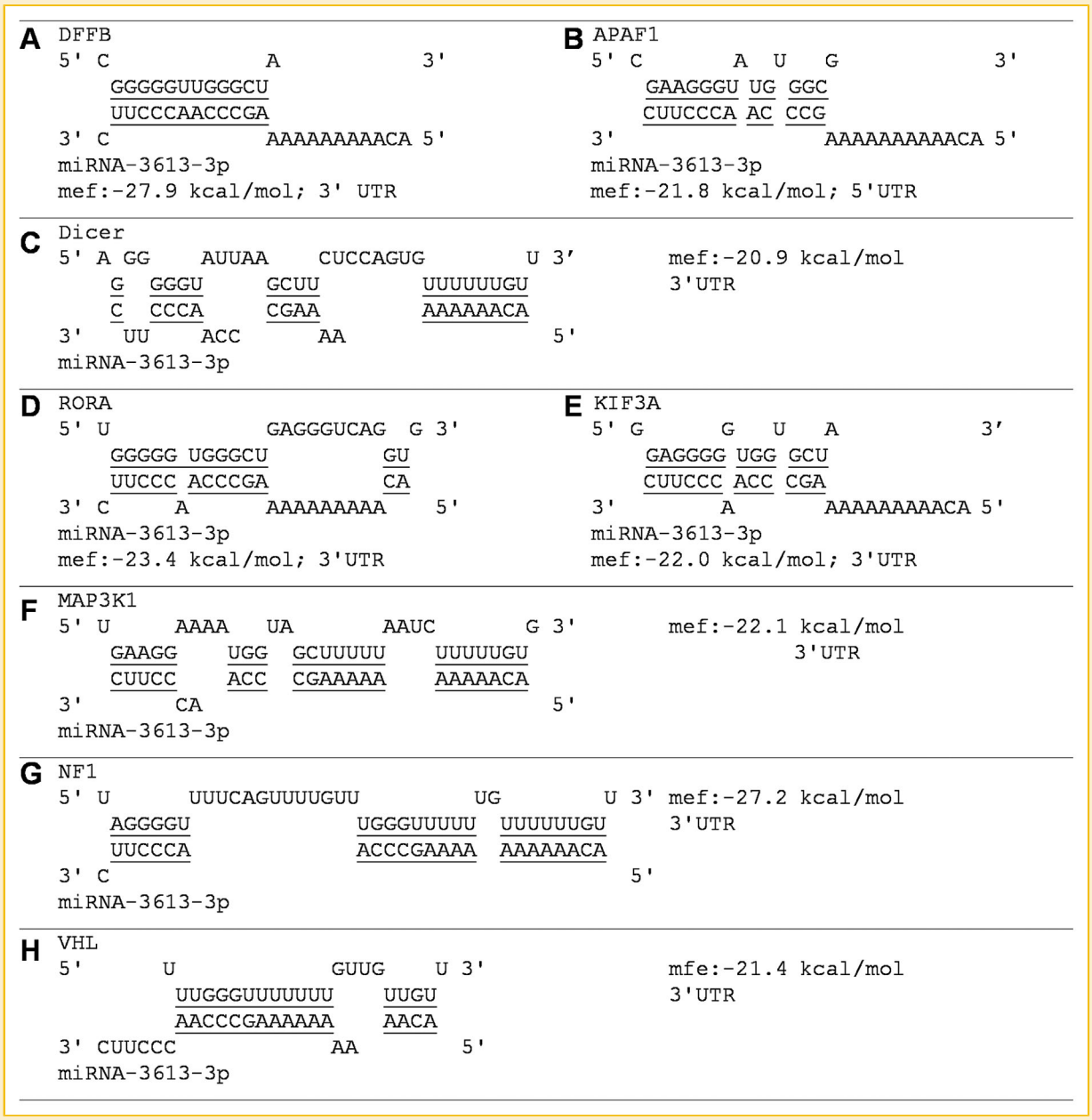


**Fig. 6.** Visualization of complementarity regions between miRNA-3613-3p and its predicted targets. Visualization of fitting between miR-3613-3p sequence and its predicted target genes: *DFFB* (A), *APAF1* (B), *DICER* (C), *RORA* (D), *KIF3A* (E), *MAP3K1* (F), *NF1* (G), and *VHL* (H) were shown. Calculation of binding energy values is presented in kcal/mol. Fitting was performed with RNAhybrid tool. Mef: minimum free energy.

therefore, MCPIP1 overexpresion-induced decline in *MCM10* mRNA content further supports our conclusion on the inhibitory effect of MCPIP1 on neuroblastoma cells.

CD248 (endosialin) present in tumor vasculature with predominant expression in pericytes in such highly malignant, MYCN-amplified, tumors as neuroblastoma, small cell lung cancer, and melanoma, has recently emerged as a potential therapeutic target [Rouleau et al., 2011]. Endosialin has epidermal growth factor and thrombomodulin domains, suggesting a role in protein–protein interaction. Therefore, the protein may play a role in cell–cell adhesion and in adhesion to extracellular matrix. We find significant decrease in the *CD248* mRNA content in MCPIP1 overexpressing neuroblastoma cells, which suggests that MCPIP1 overexpression might exert antitumor activity. CD248 is also expressed in all six human neuroblastoma cell lines (Łastowska M. personal communication).

Several distinct choline transport systems operate in the same organ to transport choline, depending on the intended fate of choline. The choline transporter CTL-1, encoded by the *SLC44A1* gene, is one of three different choline transporter systems, i.e., a

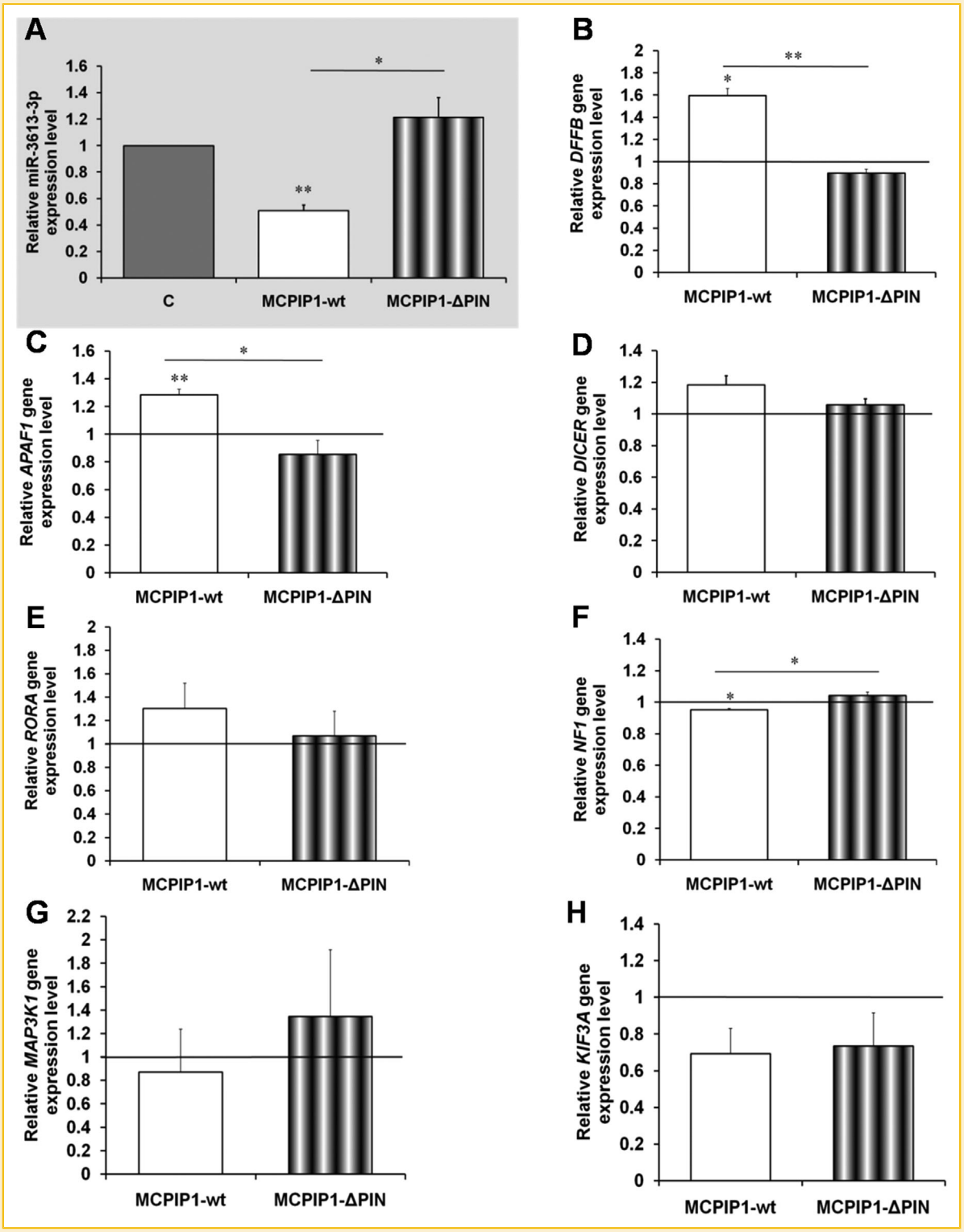


Fig. 7. Quantitative analysis of miR-3613-3p and its possible targets at their mRNA levels. A: qRT-PCR analysis of miRNA-3613-3p levels in BE(2)-C pools of control (C), expressing either wild type (MCPIP1-wt) or mutant MCPIP1 (MCPIP1-ΔPIN) cells. The reference RNA was U6snRNA. B–H: qRT-PCR analysis of seven target mRNAs: *DFFB* (B), *APAF1* (C), *DICER* (D), *RORA* (E), *NF1* (F), *MAP3K1* (G), and *KIF3A* (H). The reference RNA was *EF2*. Data on the graphs are presented as means ± SEM and calculated versus control values set as 1 (black baseline or gray bar). At least three independent experiments in triplicates were performed. *P*-values for *t*-test (control vs. MCPIP1-wt or MCPIP1-ΔPIN and MCPIP1-wt vs. MCPIP1-ΔPIN) were $P < 0.05$ (*), $P < 0.01$ (**). *P*-values for *t*-test MCPIP1-wt versus MCPIP1-ΔPIN are underlined.

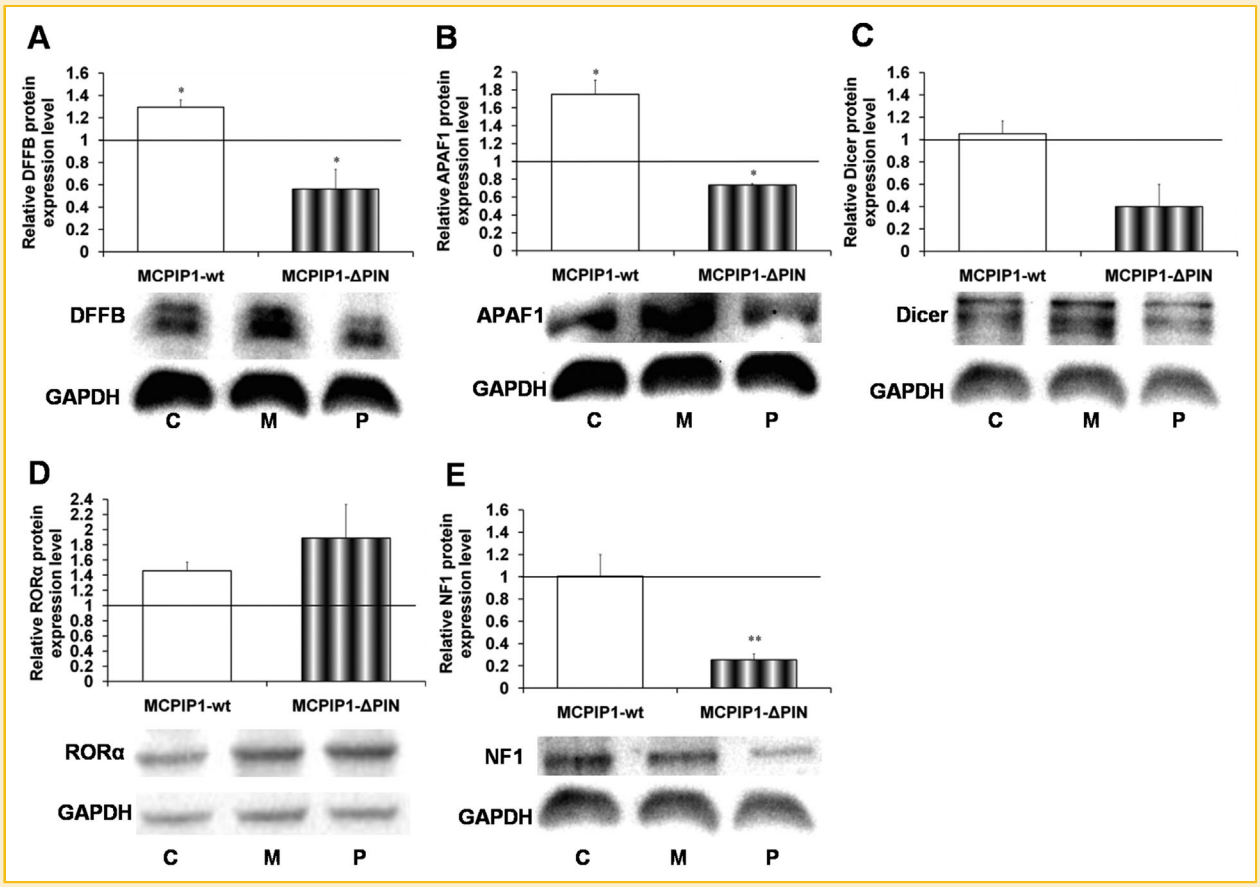


Fig. 8. Quantitative analysis of miR-3613-3p targets at their protein level. Relative DFFB (A), APAF1 (B), Dicer (C), RORα (D), and NF1 (E) proteins expression levels were measured by western blot in whole cell protein extracts from BE(2)-C pools of control (C), expressing either wild type (MCPIP1-wt) or mutant MCPIP1 (MCPIP1-ΔPIN) cells. GAPDH protein expression was used as a reference. Experiments were performed three times. Data on the graphs are presented as means ± SEM and calculated versus control values, set as 1 (black baseline). All shown western photographs were representative. *P*-values for *t*-test (control vs. MCPIP1-wt or MCPIP1-ΔPIN and MCPIP1-wt vs. MCPIP1-ΔPIN) were $P < 0.05$ (*), $P < 0.01$ (**). No significance was found for *t*-test MCPIP1-wt versus MCPIP1-ΔPIN.

high-affinity choline transporter (CTH), polyspecific organic cation transporter (OCT), and choline transporter-like protein 1 (CTL1). They belong to a family of *SLC* genes (solute carrier family) encoding transmembrane proteins responsible for transport of nutrients into cells [Wang et al., 2007]. Aberrant activation of the PI3K/Akt/mTOR pathway was also found in neuroblastoma [Iżycka-Świeżewska et al., 2010]; therefore, it can be anticipated that choline transport is enhanced in the neuroblastoma cells as it was shown for human lung adenocarcinoma [Wang et al., 2007]. Impaired choline transport found buy us in conditions of increased MCPIP1 expression may have impact on neuroblastoma cells metabolism. Thus, we can conclude that analyses of transcriptome of the BE(2)-C cells overexpressing the *MCPIP1* gene extend our knowledge on mechanism of action of MCPIP1 on the cell line. It would be interesting to evaluate genes affected by MCPIP1 overexpression in other neuroblastoma cell lines.

MicroRNA signature and expression of Dicer and Drosha can predict prognosis and delineate the risk groups in neuroblastoma [Lin et al., 2010]. An inverted correlation between MCPIP1 expression and Dicer function was observed in human lung cancer, in which a low expression of Dicer and high level of MCPIP1 are associated with poor prognosis [Suzuki et al., 2011]. Therefore, it can be postulated that MCPIP1 could be a prognostic marker in cancer. It was recently shown by others that anti-dicer RNase activity of MCPIP1 is critical for inducing angiogenesis through inhibition of production of the antiangiogenic microRNA-20b and microRNA-34a that repress the translation of hypoxia-inducible factor (HIF1α) and silent information regulator (SIRT-1), respectively [Roy et al., 2013]. In the BE(2)-C human neuroblastoma cell line, high expression of the *MCPIP1* gene correlated with impaired viability and proliferation [Skalniak et al., 2014a], however, in our model, Dicer function was not evaluated. We found that Dicer mRNA and protein levels were insignificantly increased in MCPIP1-wt-over-expressing cells. Unexpectedly, Dicer expression was severely repressed in MCPIP1-ΔPIN-overexpressing mutant, indicating involvement of the deubiquitinase supporting function of the protein. Further research is warranted on the two proteins interactions.

Interestingly, there has already been identified one microRNA targeting MCPIP1, the highly conserved microRNA-9 (miR-9), with

the well-established role in proliferation/migration of neuronal precursors and axon extension. It participates in the microglial inflammatory response via down-regulation of MCPIP1 expression, involving signalling via the NF-κB pathway but not the β-catenin pathway [Yao et al., 2014]. It was recently shown that miR-9 can be directly induced by MYCN [Ma et al., 2010]. Moreover, miR-9-mediated suppression of MCPIP1 in osteoarthritis pathogenesis might promote upregulation of IL-6 in IL-1β-stimulated human chondrocytes [Makki et al., 2015].

Enforced expression of the *MCPIP1* gene in neuroblastoma cells affected fairly small group of miRNAs, among them miR-3613-3p was found by us to be repressed in MCPIP-overexpressing BE(2)-C cells. Biological processes in which the predicted miRNA-3613-3p gene targets are involved encompass transcription factor binding and activity, ubiquitin-protein ligase activity, regulation of transcription, positive regulation of cell proliferation, metal ion binding, and regulation of protein metabolic process [Liu et al., 2014]. MiR-3613-3p is potentially involved in several important biological processes and functional pathways associated with cardiovascular pathology [Liu et al., 2014].

The predicted miRNA–mRNA interactions may contain many false positives, therefore, the functionality of such interactions needs to be verified experimentally. We have measured protein level of selected predicted miR-3613-3p targets such as *DFFB, APAF1*, *DICER*, *RORα*, and *NF1*. More detailed analysis of the genes revealed members of apoptotic machinery (*APAF1*, *DFFB*), involved in mTOR pathway (*DICER*) and also genes which are known as prognostic factors, markers of suppression and differentiation like *NF1*. Interestingly, we found that NF1, neurofibromin 1, a tumor suppressor, is not reduced (Figs. 7F and 8E), which is in agreement with other data showing that loss of NF1 in combination with overexpression of MYCN, resulted in reduced latency and increased penetrance for tumors [Huang and Weiss, 2013]. Conspicuous decrease in the NF1 protein content in BE(2)-C overexpressing the mutant of MCPIP1, devoid of the RNase domain, requires further studies as the transcript is not changed (Figs. 7F and 8E). Although direct cleavage evidence is not presented in the study, the obtained results allow to hypothesize that the expression of miR-3613-3p might be regulated by MCPIP1 by cleavage of its precursor form, but this requires experimental confirmation.

The PIN domain-defective mutant of MCPIP1 is characterized not only by its loss of ribonucleolytic activity but also by inhibition of NF-κB pathway activity [Wang et al., 2015]. At present, it is difficult to explain an influence of the mutant form of MCPIP1 in our model as only ribonucleolytic and deubiquitinase activities of this multidomain protein were partially characterized.

In summary, based on presented data, we gathered more information on effects of MCPIP1 on BE(2)-C neuroblastoma cells and found new potential gene targets as well as microRNAs for further studies.

## ACKNOWLEDGEMENTS

The study was supported by grant no. 2011/03/B/NZ1/00024 from the Polish National Science Center and grant no. 1/2014 from Research Project Competition for Young Researchers and PhD Students of the Faculty of Biochemistry, Biophysics and Biotechnology Jagiellonian University. Faculty of Biochemistry, Biophysics and Biotechnology of the Jagiellonian University is a partner of the Leading National Research Center (KNOW) supported by the Ministry of Science and Higher Education.

## REFERENCES

Adamsen D, Ramaekers V, Ho HT, Britschgi C, Rufenacht V, Meili D, Bobrowski E, Philippe P, Nava C, Van Maldergem L, Bruggmann R, Walitza S, Wang J, Grunblatt E, Thony B. 2014. Autism spectrum disorder associated with low serotonin in CSF and mutations in the SLC29A4 plasma membrane monoamine transporter (PMAT) gene. Mol Autism 5:43.

Chen Y, Stallings RL. 2007. Differential patterns of microRNA expression in neuroblastoma are correlated with prognosis, differentiation and apoptosis. Cancer Res 67:976–983.

Giraudi PJ, Bellarosa C, Coda-Zabretta CD, Peruzzo P, Tiribelli C. 2011. Functional induction of the cystine-glutamate exchanger System $Xc^-$ activity in SH-SY5Y cells by unconjugated bilirubin. PLoS ONE 6:e29078.

Grover A, Singh R, Shandilya A, Priyandoko D, Agrawal V, Bisaria VS, Wadhwa R, Kaul SC, Sundar D. 2012. Ashwagandha derived withanone targets TPX2-Aurora A complex: Computational and experimental evidence to its anticancer activity. PLoS ONE 7(1):e30890.

Guo X, Li H, Fei F, Liu B, Li X, Yang H, Chen Z, Xing J. 2015. Genetic variations in SLC3A2/CD98 gene as prognosis predictors in non-small cell lung cancer. Mol Carcinog 54:E52–E60.

Hernández-Hernández O, Sicot G, Dinca DM, Huguet A, Nicole A, Buée L, Munnich A, Sergeant N, Gourdon G, Gomes-Pereira M. 2013. Synaptic protein dysregulation in myotonic dystrophy type 1: Disease neuropathogenesis beyond missplicing. Rare Dis 1:e25553.

Horwacik I, Durbas M, Boratyn E, Wegrzyn P, Rokita H. 2013. Targeting GD2 ganglioside and aurora A kinase as a dual strategy leading to cell death in cultures of human neuroblastoma cells. Cancer Lett 341:248–264.

Huang M, Weiss WA. 2013. Neuroblastoma and MYCN. Cold Spring Harb Perspect Med 3:a014415.

Iorio E, Mezzanzanica D, Alberti P, Spadaro F, Ramoni C, D'Ascenzo S, Millimaggi D, Pavan A, Dolo V, Canevari S, Podo F. 2005. Alterations of choline phospholipid metabolism in ovarian tumor pregression. Cancer Res 65:9369–9376.

Iżycka-Świeżewska E, Drożyńska E, Rzepko R, Kobierska-Gulida G, Grajkowska W, Perek D, Balcerska A. 2010. Analysis of PI3K/AKT/mTOR signalling pathway in high risk neuroblastic tumours. Pol J Pathol 4:192–198.

Jafari N, Dogaheh HP, Bohlooli S, Oyong GG, Shirzad Z, Alibeiki F, Asl SH, Zargar SJ. 2013. Expression levels of microRNA machinery components Drosha, Dicer and DGCR8 in human (AGS, HepG2, and KEYSE-30) cancer cell lines. Int J Clin Exp Med 6:269–274.

Jansen BJ, van Ruissen F, Cerneus S, Cloin W, Bergers M, van Erp PE, Schalkwijk J. 2003. Tumor necrosis factor related apoptosis inducing ligand triggers apoptosis in dividing but not in differentiating human epidermal keratinocytes. J Invest Dermatol 121:1433–1439.

Jura J, Skalniak Ł, Koj A. 2012. Monocyte-chemotactic protein-1-induced protein-1 (MCPIP1) is a novel multifunctional modulator of inflammatory reactions. Biochim Biophys Acta 1823:1905–1913.

Kang J, Rychahou PG, Ishola TA, Mourot JM, Evers BM, Chung DH. 2008. N-myc is a novel regulator of PI3K-mediated VEGF expression in neuroblastoma. Oncogene 27:3999–4007.

Kaur M, Khan MM, Kar A, Sharma A, Saxena S. 2012. CRL4-DDB1-VPRBP ubiquitin ligase mediates the stress triggered proteolysis of Mcm10. Nucleic Acids Res 40:7332–7346.

Koppen A, Ait-Aissa R, Koster J, van Sluis PG, Ora I, Caron HN, Volckmann R, Versteeg R, Valentijn LJ. 2007. Direct regulation of the minichromosome maintenance complex by MYCN in neuroblastoma. Eur J Cancer 43:2413–2422.

Lee K-Y, Li M, Manchanda M, Batra R, Charizanis K, Mohan A, Warren SA, Chamberlain CM, Finn D, Hong H, Ashraf H, Kasahara H, Ranum LPW, Swanson MS. 2013. Compund loss of muscleblind-like function in myotonic dystrophy. EMBO Mol Med 5:1887–1900.

Li M, Cao W, Liu H, Zhang W, Liu X, Cai Z, Guo J, Wang X, Hui Z, Zhang H, Wang J, Wang L. 2012. MCPIP1 down-regulates IL-2 expression through an ARE-independent pathway. PLoS ONE 7:e49841.

Lin RJ, Lin YC, Chen J, Kuo HH, Chen YY, Diccianni MB, London WB, Chang CH, Yu AL. 2010. MicroRNA signature and expression of Dicer and Drosha can predict prognosis and delineate risk groups in neuroblastoma. Cancer Res 70:7841–7850.

Lin RJ, Chu JS, Chien HL, Tseng CH, Ko PC, Mei YY, Tang WC, Kao YT, Cheng HY, Liang YC, Lin SY. 2014. MCPIP1 suppresses hepatitis C virus replication and negatively regulates virus-induced proinflammatory cytokine responses. J Immunol 193:4159–4168.

Lipert B, Węgrzyn P, Sell H, Eckel J, Winiarski M, Budzynski A, Matlok M, Kotlinowski J, Ramage L, Malecki M, Wilk W, Mitus J, Jura J. 2014. Monocyte chemoattractant protein-induced protein 1 impairs adipogenesis in 3T3-L1 cells. Biochim Biophys Acta 1843:780–788.

Liu S, Qiu C, Miao R, Zhou J, Lee A, Liu B, Lester SN, Fu W, Zhu L, Zhang L, Xu J, Fan D, Li K, Fu M, Wang T. 2013. MCPIP1 restricts HIV infection and is rapidly degraded in activated CD4+ T cells. PNAS 110:19083–19088.

Liu H, Chen G, Liang M, Qin H, Rong J, Yao J, Wu Z. 2014. Atrial fibrillation alters the microRNA expression profiles of the left atria of patients with mitral stenosis. BMC Cardiovasc Disord 14:10.

Lyu JH, Park DW, Huang B, Kang SH, Lee SJ, Lee C, Bae YS, Lee JG, Baek SH. 2015. RGS2 suppresses breast cancer cell growth via a MCPIP1-dependent pathway. J Cell Biochem 116:260–267.

Ma L, Young J, Prabhala H, Pan E, Mestdagh P, Muth D, Teruya-Feldstein J, Reinhardt F, Onder TT, Valastyan S, Westermann F, Speleman F, Vandesompele J, Weinberg RA. 2010. MiR-9, a MYC/MYCN-activated microRNA, regulates E-cadherin and cancer metastasis. Nat Cell Biol 12:247–256.

Makki MS, Haseeb A, Haggi TM. 2015. MicroRNA-9 promotes IL-6 expression by inhibiting MCPIP1 expression in IL-1β-stimulated human chondrocytes. Arthritis Rheumatol 67:2117–2128.

Matsushita K, Takeuchi O, Standley DM, Kumagai Y, Kawagoe T, Miyake T, Satoh T, Kato H, Tsujimura T, Nakamura H, Akira S. 2009. Zc3h12a is an RNase essential for controlling immune responses by regulating mRNA decay. Nature 458:1185–1190.

Michel V, Bakovic M. 2012. The ubiquitous choline transporter SLC44A1. Cent Nerv Syst Agents Med Chem 12:70–81.

Mizgalska D, Wegrzyn P, Murzyn K, Kasza A, Koj A, Jura J, Jarząb B, Jura J. 2009. Interleukin-1-inducible MCPIP protein has structural and functional properties of RNase participating in degradation of IL-1-mRNA. FEBS J 276:7386–7399.

Odawara H, Iwasaki T, Horiguchi J, Rokutanda N, Hirooka K, Miyazaki W, Koibuchi Y, Shimokawa N, Iino Y, Takeyoshi I, Koibuchi N. 2009. Activation of aromatase expression by retinoic acid receptor-related orphan receptor (ROR) alpha in breast cancer cells: Identification of a novel ROR response element. J Biol Chem 284:17711–17719.

Okorokov AL, Waugh A, Hodgkinson J, Murphy A, Hong HK, Leo E, Sherman MB, Stoeber K, Orlova EV, Williams GH. 2007. Hexameric ring structure of human MCM10 DNA replication factor. EMBO Reports 8:925–930.

Ora I, Eggert A. 2011. Progress in treatment and risk stratification of neuroblastoma: Impact on future clinical and basic research. Semin Cancer Biol 21:217–228.

Ray B, Simon JR, Lahiri DK. 2009. Determination of high-affinity choline uptake (HACU) and choline acetyltransferase (ChAT) activity in the same population of cultured cells. Brain Res 1297:160–168.

Robles AI, Bemmels NA, Foraker AB, Harris CC. 2001. APAF-1 is a transcriptional target of p53 in DNA damage-induced apoptosis. Cancer Res 61:6660–6664.

Rouleau C, Smale R, Sancho J, Fu Y-S, Kurtzberg L, Weber W, Kruger A, Jones C, Roth S, Bormann C, Dunham S, Krumbholz R, Curiel M, Wallar G, Mascarello J, Campos-Rivera J, Horten B, Schmid S, Miller G, Teicher BA. 2011. Endosialin: A novel malignant cell therapeutic target for neuroblastoma. Int J Oncol 39:841–851.

Roy A, Zhang M, Saad Y, Kolattukudy PE. 2013. Antidicer RNAse activity of monocyte chemotactic protein-induced protein-1 is critical for inducing angiogenesis. Am J Physiol Cell Physiol 305:C1021–C1032.

Skalniak L, Mizgalska D, Zarebski A, Wyrzykowska P, Koj A, Jura J. 2009. Regulatory feedback loop between NF-kappaB and MCP-1-induced protein 1 RNase. FEBS J 276:5892–5905.

Skalniak L, Koj A, Jura J. 2013. Proteasome inhibitor MG-132 induces MCPIP1 expression. FEBS J 280:2665–2674.

Skalniak L, Dziendziel M, Jura J. 2014. MCPIP1 contributes to the toxicity of proteasome inhibitor MG-132 in HeLa cells by the inhibition of NF-κB. Mol Cell Biochem 395:253–263.

Skalniak A, Boratyn E, Tyrkalska SD, Horwacik I, Durbas M, Łastowska M, Jura J, Rokita H. 2014a. Expression of the monocyte chemotactic protein-1-induced protein 1 decreases human neuroblastoma cell survival. Oncol Rep 31:2385–2392.

Smith PK. 1985. Measurement of protein using bicinchoninic acid. Anal Biochem 150:76–85.

Stroynowska-Czerwińska A, Fiszer A, Krzyżosiak WJ. 2014. The panorama of miRNA-mediated mechanisms in mammalian cells. Cell Mol Life Sci 71:2253–2270.

Suzuki HI, Arase M, Matsuyama H, Choi YL, Ueno T, Mano H, Sugimoto K, Miyazono K. 2011. MCPIP1 ribonuclease antagonizes Dicer and terminates microRNA biogenesis through precursor microRNA degradation. Molecular Cell 44:424–436.

Thorell K, Bergman A, Caren H, Nilsson S, Kogner P, Martinsson T, Abel F. 2009. Verification of genes differentially expressed in neuroblastoma tumours: A study of potential tumour suppressor genes. BMC Med Genomics 2:53.

Vrotsos EG, Kalattukudy PE, Sugaya K. 2009. MCP-1 involvement in glial differentiation of neuroprogenitor cells through APP signaling. Brain Res Bull 79:97–103.

Wang T, Li J, Chen F, Zhao Y, He X, Wan D, Gu J. 2007. Choline transporters in human lung adenocarcinoma: expression and functional implications. Acta Biochim Biophys Sinica 39:668–674.

Wang W, Huang X, Xin HB, Fu M, Xue A, Wu ZH. 2015. TRAF family member-associated NF-κB activator (TANK) inhibits genotoxic nuclear factor κB activation by facilitating deubiquitinase USP10-dependent deubiquitination of TRAF6 ligase. J Biol Chem 290:13372–13385.

Xu W, Yang X, Hu X, Li S. 2014. Fifty-four novel mutations in the NF1 gene and integrated analyses of the mutations that modulate splicing. Int J Mol Med 34:53–60.

Yao H, Ma R, Yang L, Hu G, Chen X, Duan M, Kook Y, Niu F, Liao K, Fu M, Hu G, Kolattukudy P, Buch S. 2014. MiR-9 promotes microgial activation by targeting MCPIP1. Nature Commun 5:4386.

Zhi F, Wang R, Wang Q, Xue L, Deng D, Wang S, Yang Y. 2014. MicroRNAs in neuroblastoma: Small-sized players with a large impact. Neurochem Res 39:613–623.